

Syntheses and Structures of Three Types of Hybrid Metal Dipicolinato Complexes Induced by Alkali Metal Ion and the Semiconductor Character

Chengbing Ma, Changneng Chen, Feng Chen, Xiaofeng Zhang, Hongping Zhu, Qiutian Liu,* Daizheng Liao,† and Licun Li†

State Key Laboratory of Structural Chemistry, Fujian Institute of Research on the Structure of Matter, Chinese Academy of Sciences, Fuzhou 350002, China

†Department of Chemistry, Nankai University, Tianjing 300071, China

(Received July 15, 2002)

Three types of hybrid transition-alkali metal complexes, $[MK_2(pdc)_2(H_2O)_7]_n$ (H_2pdc = 2,6-pyridinedicarboxylic acid, or so-called dipicolinic acid, M = Mn (**1**), Co (**2**), Zn (**3**), $Mn_{0.5}Co_{0.5}$ (**4**)), $\{[Na_2(H_2O)_8(CH_3OH)_{0.5}][Mn_2Na_2(pdc)_4(H_2O)_8]\cdot 0.25CH_3OH\cdot 2H_2O\}_n$ (**5**) and $[Ni(H_2O)_6][Ni_2K_2(pdc)_4(H_2pdc)_2(H_2O)_2]\cdot 2H_2O$ (**6**) were self-assembled from a reaction system containing a divalent transition metal, alkali metal and H_2pdc, and were isolated under different crystallization conditions. In all complexes, $[M(pdc)_2]^{2-}$ units were included as independent components to connect to the alkali metal chains or pdc units. Alkali metal ions act as templates for inducing the organization of the $[M(pdc)_2]^{2-}$ components into respective special architectures in different fashions. Complexes **1**–**4** are isostructural with the same space group and similar cell parameters, in which the $[M(pdc)_2]^{2-}$ units are bonded to the water-bridged K chains forming neutral 2D lamellar-like polymers, while **5** contains water-bridged Na chains correlated to Mn_2Na_2 cluster anions by hydrogen bonds, and **6** is a discrete Ni_2K_2 tetranuclear cluster consisting of $Ni(pdc)_2$ and $K(H_2pdc)$ units. The infrared spectra of these complexes show a large difference between the asymmetrical and symmetrical stretching vibrations, $\Delta(\nu_{as} - \nu_s) > 200\ cm^{-1}$, for the carboxyl groups, indicating unidentate and unsymmetrical bridging coordination modes. The variable-temperature electrical conductivities of complexes **1**–**5** were determined to display semiconductor features, and the magnetic properties of **1**, **2**, **4** and **5** were also studied.

Extensive research attention has been paid to the design and synthesis of transition-metal complexation by dipicolinic acid due to its versatile, yet unpredictable, coordination modes, such as bidentate,[1] terdentate[2] and bridging,[3] and its interesting properties, such as diverse biological activity,[4] and an ability to stabilize unusual oxidation states,[5] as well as its application to a diverse area of technology.[6] On the other hand, the chemistry of heteropolymetallic complexes has been a hot subject on account of its intriguing magnetic interactions between metal centers,[7] its relevance to the active site of multimetalloenzymes,[8] and its potential as a functional solid material.[9]

Template synthesis is commonly used to product a regular metal-ligand framework,[10] and a number of such compounds have been generated to show how an assembly of metal ions and organic components can be successfully induced by counterions.[11] However, the cases on metal ions, particularly hard metal ions as template agents, are relatively rare.[12] This work reports on systematical reactions of divalent transition metal (Mn, Co, Zn, Ni) salts with dipicolinic acid in the presence of alkali metal (Na or K) hydrate as a template reagent to induce assembly. Three types of hybrid transition metal-alkali metal dipicolinato complexes possessing respective special architectures and interesting properties are also included.

Results and Discussion

Structures. Complexes 1–4: Because the four complexes are isostructural with each other, as confirmed by X-ray diffraction, only the structure of **1** is described as being a representative. Selected bond lengths of these complexes and the angles of **1** are listed in Table 1. Neutral polymer **1** possesses the simplest unit of $[MnK_2(pdc)_2(H_2O)_7]$, composed of two subunits, $[K_2(\mu\text{-}H_2O)_2(H_2O)_5]^{2+}$ and $[Mn(pdc)_2]^{2-}$, as shown in Fig. 1. In the structure of $[K_2(\mu\text{-}H_2O)_2(H_2O)_5]^{2+}$, the potassium centers exhibit six or seven-coordinate environments consisting of two bridging carboxyl O atoms, as well as two bridging and two or three terminal water molecules. It is noticed that the mean $K\text{–}O_{pdc}$ distance of 2.82 Å (K2–O1, 2.7075(1) Å; K1–O1, 2.9359(2) Å) is shorter than that of the mean $K\text{–}O_{aqua}$ of 2.91 Å (K1–O5, 2.8027(2) Å; K2–O5, 3.0202(2) Å), indicating that the carboxyl O bridges may play a more important role in stabilizing the $[K_2(\mu\text{-}O_{aqua})_2(\mu\text{-}O_{pdc})_2(H_2O)_5]_n$ chain (K chain), as shown in Fig. 2. The separations between potassium ions of 4.09–4.17 Å for **1**–**4** are smaller than the sum of the van der Waals radii, implying a possible weak intermetallic interaction.[13] In the structure of $[Mn(pdc)_2]^{2-}$, the Mn(II) ion is chelated by two terdentate pdc ligands to form a strongly dis-

Table 1. Selected Bond Lengths (Å) of **1**–**4** and Angles (°) of **1**

	1, M = Mn	**2**, M = Co	**3**, M = Zn	**4**, M = 0.5(Mn + Co)
M–N	2.1625(2)	2.028(2)	2.015(3)	2.088(2)
M–O3	2.2169(1)	2.1597(18)	2.170(2)	2.1835(18)
M–O2	2.2287(1)	2.1662(17)	2.195(3)	2.1891(19)
K1–O5	2.8027(2)	2.799(2)	2.803(3)	2.798(2)
K1–O6	2.9171(3)	2.8838(19)	2.889(3)	2.9060(19)
K1–O1	2.9359(1)	2.979(3)	2.961(4)	2.910(4)
K1···K2	4.1693(4)	4.1279(5)	4.1140(7)	4.1447(5)
K2–O8	2.6651(4)	2.663(5)	2.661(7)	2.661(5)
K2–O1	2.7075(1)	2.7467(18)	2.723(3)	2.7295(19)
K2–O7	2.8021(2)	2.795(2)	2.803(3)	2.797(2)
K2–O5	3.0202(1)	2.960(2)	2.954(3)	2.985(2)
		Selected Angles of **1**		
N#1–Mn–N	166.80(8)		O6–K1–O8#3	130.69(8)
N–Mn–O3	72.70(5)		O1–K1–O8#3	64.82(1)
N–Mn–O3#1	117.41(5)		O5–K1–O8#4	90.78(2)
O3–Mn–O3#1	89.67(7)		O6–K1–O8#4	58.53(1)
N–Mn–O2#1	97.95(5)		O1–K1–O8#4	130.07(1)
O3–Mn–O2#1	101.22(6)		O8–K2–O1	86.01(16)
N–Mn–O2	72.42(5)		O1#3–K2–O1	161.42(7)
O3–Mn–O2	144.63(5)		O8–K2–O7#3	145.37(17)
O2#1–Mn–O2	89.17(8)		O1–K2–O7#3	90.02(5)
O5#2–K1–O5	83.99(7)		O7#3–K2–O7	82.41(8)
O5–K1–O6#2	124.96(5)		O8–K2–O5	86.92(16)
O5–K1–O6	81.09(5)		O1–K2–O5	78.79(4)
O6#2–K1–O6	147.32(8)		O7–K2–O5	141.01(6)
O5–K1–O1	78.78(4)		O8–K2–O5#3	73.51(16)
O6–K1–O1	71.61(5)		O1–K2–O5#3	98.02(5)
O5–K1–O1#2	153.88(5)		O7–K2–O5#3	58.61(5)
O6–K1–O1#2	92.83(5)		O5–K2–O5#3	160.37(7)
O1–K1–O1#2	123.53(6)		K2–O1–K1	95.17(4)
O5–K1–O8#3	69.11(1)		K1–O5–K2	91.37(5)
K2–O8–K1#3	90.36(1)			

Symmetry codes: #1, x, $-y + 3/2$, $-z + 1/2$; #2, x, $-y + 3/2$, $-z - 1/2$; #3, $-x + 3/2$, $-y + 1$, z; #4, $-x + 3/2$, $y + 1/2$, $-z - 1/2$.

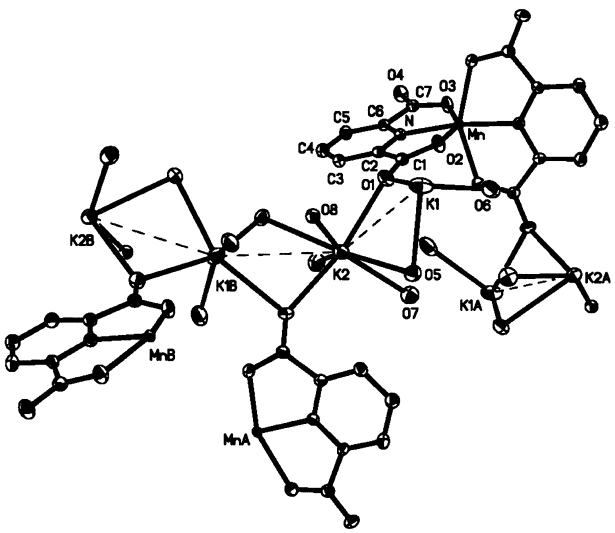

Fig. 1. Structure of **1** with selected atom-labeling scheme showing a $[MnK_2(pdc)_2(H_2O)^7]$ unit and the extension of the unit along *bc* plane. All hydrogen atoms are omitted for clarity.

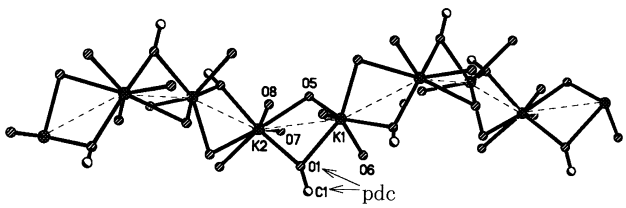

Fig. 2. A view of 1-D $[K_2(\mu\text{-}H_2O)(\mu\text{-}O_{carboxyl})]$ chain in **1** showing the coordination environments of K centers. Hydrogen atoms are omitted for clarity.

torted octahedron with the following axial angles: N–Mn–N# (#: x, $-y + 3/2$, $-z + 1/2$) of 166.80(8)° and O3–Mn–O2 of 144.63(5)°, and other angles ranging from 72.42(5)° to 117.41(5)°. The basic $[MnK_2(pdc)_2(H_2O)_7]$ units develop along the crystallographic bc plane to form a 2D lamellar structure, as shown in Fig. 3, in which $[Mn(pdc)_2]^{2-}$ fragments lie between parallel K-chains and link the K-chains by carboxyl O atoms. Taking vividly sinusoid-like features, the K-chains wind their way between the $[Mn(pdc)]^{2-}$ units with an interchain separation of 8.159 Å, and display a template effect of inducing a regular arrangement of $[Mn(pdc)]^{2-}$ fragments

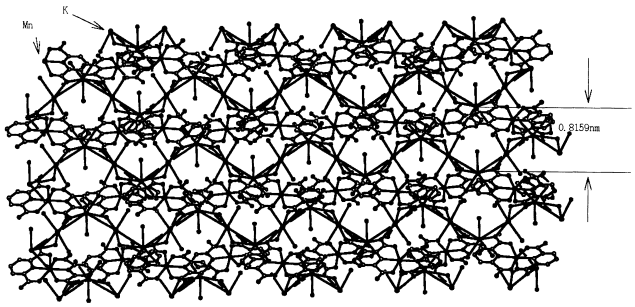

Fig. 3. View of the lamellar structure of **1** showing the $[Mn(pdc)_2]^{2-}$ units alternately located at both the sides of the K chain. The sinusoid-like K chains are embedded between two adjacent arrays of Mn units with the separation of 8.159 Å in the *bc* plane.

Table 2. Parameters (Å, °) for Hydrogen-Bonding Interactions of **1**

D–H···A	d (D–H)	d (H···A)	< DHA	d (D···A)
O5–H5B···O3[a)]	0.865	2.009	168.06	2.861
O5–H5C···O7[b)]	0.852	2.109	146.10	2.856
O6–H6A···O2	0.835	1.906	169.06	2.730
O6–H6B···O4[c)]	0.807	1.998	167.01	2.791
O7–H7A···O6[d)]	0.836	1.970	170.59	2.798
O7–H7B···O4[e)]	0.809	2.102	171.71	2.905
O8–H8A···O6[f)]	0.861	2.562	112.12	2.994
O8–H8B···O4[g)]	0.853	2.122	166.87	2.960

Symmetry codes: a) $x + 1/2, -y + 3/2, z - 1/2$; b) $-x + 3/2, -y + 1, z$; c) $-x + 1, y + 1/2, z - 1/2$; d) $-x + 3/2, y - 1/2, -z + 1/2$; e) $-x + 1, -y + 1, -z + 1$; f) $-x + 3/2, y - 1/2, -z - 1/2$; g) $-x + 1, -y + 1, -z$.

along both sides of the chains. These 2D layers are further linked through extensive hydrogen bonds (listed in Table 2) to produce a 3D layer-stack-like supramolecular architecture with an interlayer distance of 10.61 Å.

Complex 5: As shown in Fig. 4, the structure of **5** contains a large Mn_2Na_2 cluster dianion, $[Mn_2Na_2(pdc)_4(H_2O)_8]^{2-}$, which consists of a $[Na_2(\mu\text{-}H_2O)_2(H_2O)_6]^{2+}$ dimer and two $[Mn(pdc)_2]^{2-}$ units linked together by carboxyl O atoms. The sodium dimer acts as a template to arrange two $[Mn(pdc)_2]^{2-}$ units on both sides of the dimer by the linkage of Na–O_{pdc}. The structural parameters of the $[Mn(pdc)_2]^{2-}$ fragment are very close to those in **1**–**4**, just as listed in Table 3.

There are water bridged Na chains, $[\{Na_2(\mu\text{-}H_2O)_2\}(\mu\text{-}H_2O)]_n$, outside of the center Mn_2Na_2 cluster dianions, maintaining the charge balance of the whole complex. Hydrogen-bonding interactions exist between the carboxyl groups and ligated water or solvate H_2O (O37 and O38) molecules, as shown in Fig. 4 caption. These hydrogen bonds correlate the Na chains and the Mn_2Na_2 dianions while generating a complicated-hydrogen bonding network and a 3D supramolecular framework, as shown in Fig. 5. The Na chains and the Mn_2Na_2 dianions are arrayed alternately in the structure without any direct covalent bonding interaction between them, except for hydrogen-bonding interactions. Scheme 1 simplifies the supramolecular structure of **5**, showing the structural difference between **1**–**4** and **5**: (1) Na chains do not contain oxygen atoms of pdc ligands, in contrast to the participation of pdc into the K chains for **1**–**4**; (2) Na chains contain both single and double μ-O bridges different from the K chains, which contain only double μ-O bridges, and (3) compared to the sinusoid-like feature of the K chains, the tropism of the Na chains is irregular.

Complex 6: The structure of **6** consists of a mixed Ni_2K_2 cluster dianion, $[Ni_2K_2(pdc)_4(H_2pdc)_2(H_2O)_2]^{2-}$, one counteri-

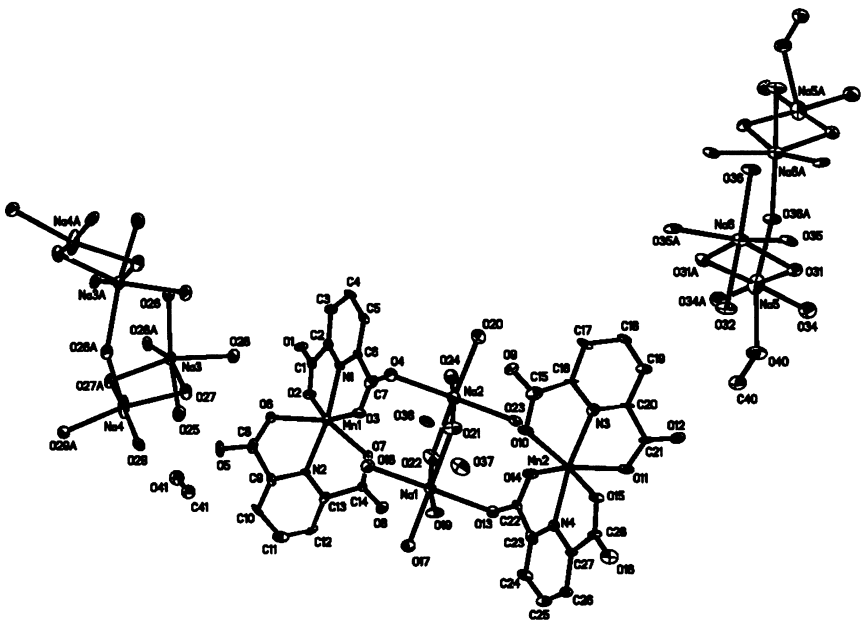

Fig. 4. ORTEP drawing of **5** with atom-labeling showing thermal ellipsoids at 30% probability. Hydrogen bonds are listed as O···O separations (Å): O5···O25, 2.810; O5···O27, 2.828; O6···O28, 2.933; O7···O38, 2.777; O24···O38, 2.754; O10···O37, 2.722; O19···O37, 2.653.

Table 3. Selected Bond Lengths (Å) and Angles (°) of **5**

Mn1–N2	2.133(7)	Na1–O19	2.344(1)
Mn1–N1	2.158(8)	Na1–O17	2.375(8)
Mn1–O3	2.214(8)	Na1–O18	2.416(9)
Mn1–O7	2.205(8)	Na1–O22	2.468(1)
Mn1–O2	2.223(9)	Na1–O21	2.476(9)
Mn1–O6	2.250(9)	Na1–O13	2.504(9)
Mn2–N4	2.143(9)	Na2–O24	2.351(1)
Mn2–O10	2.175(9)	Na2–O21	2.449(1)
Mn2–N3	2.182(9)	Na2–O23	2.457(9)
Mn2–O14	2.195(8)	Na2–O22	2.532(1)
Mn2–O15	2.248(8)	Na2–O4	2.529(1)
Mn2–O11	2.253(9)	Na2–O20	2.522(9)
N2–Mn1–N1	169.9(3)	O19–Na1–O17	88.9(4)
N2–Mn1–O3	110.9(3)	O19–Na1–O18	100.9(4)
N1–Mn1–O3	73.4(3)	O17–Na1–O18	89.1(3)
N2–Mn1–O7	72.2(3)	O19–Na1–O22	171.8(4)
N1–Mn1–O7	117.6(3)	O17–Na1–O22	98.7(4)
O3–Mn1–O7	87.3(3)	O18–Na1–O22	82.4(4)
N2–Mn1–O2	105.1(3)	O19–Na1–O21	87.1(3)
N1–Mn1–O2	71.2(3)	O17–Na1–O21	176.0(5)
O3–Mn1–O2	144.1(3)	O18–Na1–O21	91.0(3)
O7–Mn1–O2	103.9(4)	O22–Na1–O21	85.3(3)
N2–Mn1–O6	71.9(3)	O19–Na1–O13	89.3(3)
N1–Mn1–O6	98.2(3)	O17–Na1–O13	86.7(3)
O3–Mn1–O6	104.4(4)	O18–Na1–O13	168.9(4)
O7–Mn1–O6	144.1(3)	O22–Na1–O13	88.1(4)
O2–Mn1–O6	86.4(4)	O21–Na1–O13	93.9(3)
Na2–O21–Na1	96.0(4)	Na1–O22–Na2	94.1(4)

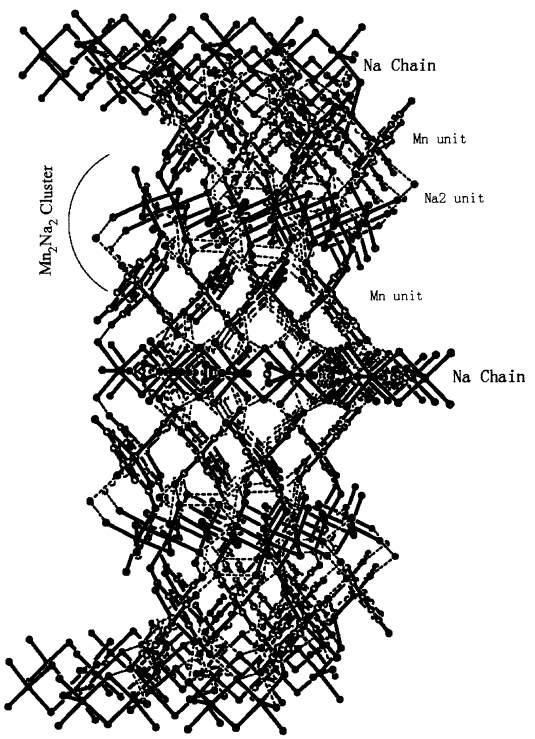

Fig. 5. Perspective view of the structure of **5** showing the 3D framework generated from hydrogen-bonding interactions (view along the *a* axis).

on, $[Ni(H_2O)_6]^{2+}$, and two solvate water molecules. Figure 6 and Table 4 show the structure of the Ni_2K_2 cluster anion and the selected bond parameters, respectively. The Ni_2K_2 cluster anion consists of two $[Ni(pdc)_2]^{2-}$ and two $[K(H_2pdc)(H_2O)]^{+}$

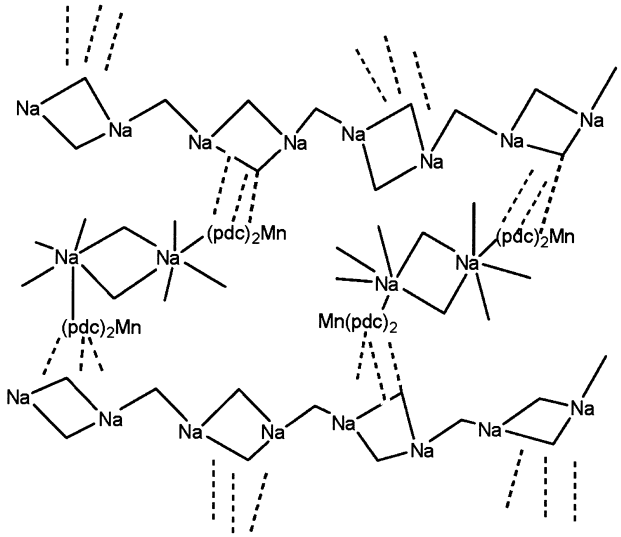

Scheme 1. Supramolecular structure scheme of **5** showing the correlation of Na chains and Mn_2Na_2 cluster units. Dot lines indicate hydrogen bonding interactions between both the components.

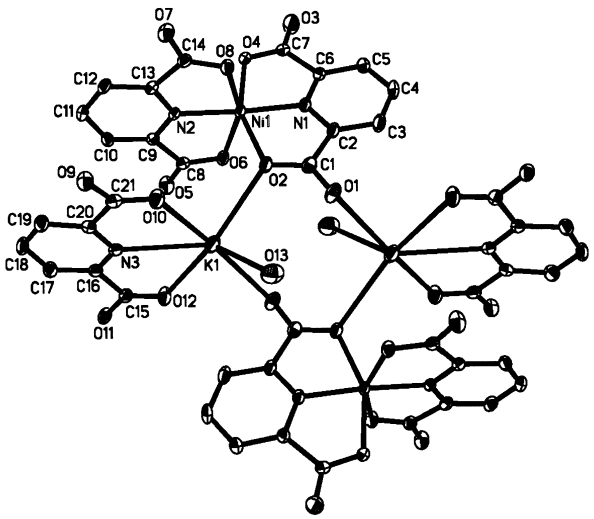

Fig. 6. ORTEP drawing of cluster anion of complex **6** with independent atom-labeling showing thermal ellipsoids at 35% probability.

subunits. The Ni(II) center displays a strongly distorted octahedral geometry like those of $[M(pdc)_2]^{2-}$ in **1**–**5**, and is chelated by two pdc^{2-} ligands with Ni–O distances in the range 2.120(3)–2.175(3) Å, Ni–N distances of 1.974(3) Å and 1.978(3) Å, and the most distorted angle, O8–Ni1–O6, of 154.01(1)°. The K center is terdenatately chelated by a neutral H_2pdc with a K–N distance of 2.889(3) Å and K–O distances of 2.734(3) and 2.938(3) Å; in addition, one water molecule (K1–O13, 2.721(4) Å) and two other carboxyl oxygen atoms from the neighboring two $[Ni(pdc)_2]^{2-}$ fragments (K1–O2, 2.958(3); K1–O1#, 2.796(3) Å; #: $-x + 1$, $-y - 1$, $-z + 1$) complete the six-coordinate structure. The positioning of the acidic H atom is based on the following: (1) The ESR spectrum confirms the Ni(II) oxidation state ($g = 2.4607$ close to

Table 4. Selected Bond Lengths (Å) and Angles (°) of **6**

Ni1–N2	1.974(3)	O1–C1	1.244(5)
Ni1–N1	1.978(3)	O2–C1	1.269(5)
Ni1–O8	2.120(3)	O3–C7	1.228(5)
Ni1–O4	2.129(3)	O4–C7	1.273(5)
Ni1–O2	2.138(3)	O5–C8	1.231(5)
Ni1–O6	2.175(3)	O6–C8	1.272(5)
K1–O13	2.721(4)	O7–C14	1.249(5)
K1–O10	2.734(3)	O8–C14	1.258(5)
K1–O1#2	2.796(3)	O9–C21	1.296(5)
K1–N3	2.889(3)	O10–C21	1.218(5)
K1–O12	2.938(3)	O11–C15	1.315(5)
K1–O2	2.958(3)	O12–C15	1.213(5)
N2–Ni1–N1	175.84(1)	O10–K1–N3	58.01(9)
N2–Ni1–O8	77.91(1)	O1#2–K1–N3	127.70(1)
N1–Ni1–O8	101.24(1)	O13–K1–O12	128.21(1)
N2–Ni1–O4	98.13(1)	O10–K1–O12	114.06(9)
N1–Ni1–O4	77.80(1)	O1#2–K1–O12	73.46(9)
O8–Ni1–O4	92.43(1)	N3–K1–O12	56.11(9)
N2–Ni1–O2	106.28(1)	O13–K1–O2	71.31(1)
N1–Ni1–O2	77.78(1)	O10–K1–O2	73.88(9)
O8–Ni1–O2	92.12(1)	O1#2–K1–O2	105.89(9)
O4–Ni1–O2	155.58(1)	N3–K1–O2	125.69(9)
N2–Ni1–O6	77.17(1)	O12–K1–O2	156.32(1)
N1–Ni1–O6	103.89(1)	O13–K1–O10	92.01(1)
O8–Ni1–O6	154.80(1)	O13–K1–O1#2	71.64(1)
O4–Ni1–O6	94.70(1)	O10–K1–O1#2	162.32(1)
O2–Ni1–O6	91.30(1)	O13–K1–N3	129.24(1)

Symmetry codes: #1 $-x + 1, -y, -z + 1$; #2 $-x + 1, -y - 1, -z + 1$.

the value reported in the literature);[14] so as to keep the electroneutrality of the compound, two protons need to be added to the pdc^{2-} ligands. (2) The strong IR absorption at 1714 cm^{-1} can be assigned to the asymmetrical stretching vibration of a protonated carboxyl group, as reported for a complex containing diacid.[15] (3) The large bond lengths of C15–O11 (1.315(5) Å) and C21–O9 (1.296(5) Å) indicate that the H atoms should be added to the O11 and O9 positions, which is also in agreement with the case of $[Zn(pdc)(H_2pdc)]\cdot 2H_2O$.[16] Four metal atoms make a parallelogram framework in which an electropositive K ion acts as a template for inducing the formation of a hetero-tetra-metal aggregate by linking electronegative carboxyl O atoms of two $[Ni(pdc)_2]^{2-}$ fragments to the K ion. Notably, as a novel mixed four-metal cluster, this complex would provide a potential for modeling a heterometal nickel-containing enzyme, and for homogeneous catalysis and molecular tools in DNA cleavage as other dipicolinato complexes.[17]

Syntheses. Complexes **1**–**6** were all generated through the self-assembly system of dipicolinic acid, alkali and transition metal ions under similar conditions. Three types of the mixed metal clusters were isolated. A common feature of all of these complexes is that transition-metal dipicolinate, $[M(pdc)_2]^{2-}$, fragments exist in these complexes as a basic structural unit. When KOH was used in the reaction, the $[M(pdc)_2]^{2-}$ fragments of complexes **1**–**4** were linked to a water-bridged alkali-metal chain. However, when NaOH was used to prepare **5**, the $[M(pdc)_2]^{2-}$ fragments only existed in the Mn_2Na_2 cluster dianions, which are independent outside of the Na/H_2O chain. Contrary to the chain structure, complex **6** formed a hetero tetranuclear, Ni_2K_2, cluster with the $[Ni(pdc)_2]^{2-}$ fragment linked by the $[K(H_2pdc)]^+$ unit. Though the results of the self-assembly are complicated and seemingly unpredictable, it is suggested that the construction of a specific architecture for these complexes may be alkali metal-ion dependent. Attempts to produce the same polymeric structure as that of **1** by substituting NaOH for KOH in the reaction did not succeed, and complex **5** was always obtained, indicating the influence of the size of the alkali metal on the structure of the resulting product. It is clear that the difference in radii of 0.35 Å between the Na^+ and K^+ ions does not allow the same type of supramolecular interactions, due to a higher steric crowding in Na^+-containing structures. Consequently, only simple Mn_2Na_2 tetranuclear moieties are produced together with independent Na chains. On the other hand, the structurally dramatic difference of **6** should be attributed to the conditions of the reaction and isolation. Water was selected as the solvent instead of an organic solvent, such as MeOH, in the preparation of **6**. The poor solubility of a metal cluster in ether/H_2O promotes the rapid deposition of small molecules, while crystallization of other complexes, **1**–**5**, in MeOH needs a prolonged time (weeks). However, the participation of alkali-metal ions is crucial to yield these special structures from a heterotetranuclear Mn_2Na_2, Ni_2K_2 cluster to supramolecular M/K complexes containing water-bridged alkali chains. According to the size of the alkali metal ion and the reaction conditions, the alkali metal ions as the template play an important role in for inducing a suitable array of $[M(pdc)_2]^{2-}$ fragments.

Infrared Spectra. All of the complexes show obvious widening peaks at ca. 3300–3550 cm^{-1}, which stem from the existence of many water molecules associated with the water-bridged alkali metal chains of complexes **1**–**5**. Complex **6** contains solvate H_2O molecules, indicated by the peaks at 3448 and 3521 cm^{-1}. It is also noted that complexes **1**–**5** display asymmetric stretching vibrations of the COO^- groups in the range from 1639 cm^{-1} to 1585 cm^{-1}, and symmetric stretching vibrations, $\nu_s(COO^-)$ from 1429 cm^{-1} to 1362 cm^{-1}. In addition to the aforementioned absorptions, complex **6** shows a high-frequency vibration at 1714 cm^{-1} (vide supra) associated with the asymmetric stretching vibration of the protonated carboxyl group. In these complexes, all of the carboxyl groups coordinate to the transition and alkali metal ions in unsymmetrical bridging (M–O–C–O–M′) and unidentate (M–O–C=O) modes, which are believed to associate with the large difference between the asymmetric and symmetric COO stretchings, $\Delta(\nu_{as} - \nu_s)$.[18] For all of these complexes, the $\Delta(\nu_{as} - \nu_s)$ values are larger than 200 cm^{-1}, which is a general indication[18] of unidentate or unsymmetrical bridging coordination. Chelating carboxyl leading to a small $\Delta(\nu_{as} - \nu_s)$ value was not found, which is also in agreement with the spectral feature for these complexes.

Electrical Conductivity. The water-bridged alkali metal chains are a common characteristic of complexes **1**–**5**. Thermogravimetic analyses (TGA) revealed these complexes as being thermally stable below 393 K. Accordingly, the electrical conductivities of **1**–**5** were measured in the temperature region between 286 and 383 K. The conductivities vary over the range from 1.18×10^{-5} to 5.26×10^{-5} S cm^{-1} at room temperature for these complexes, and take on a rising trend (Fig. 7) with increasing temperature, interestingly exhibiting semi-conductivity.[19] The corresponding activation energies were calculated to be 17.971, 6.139, 25.930, 14.883 and 8359 kJ mol^{-1},

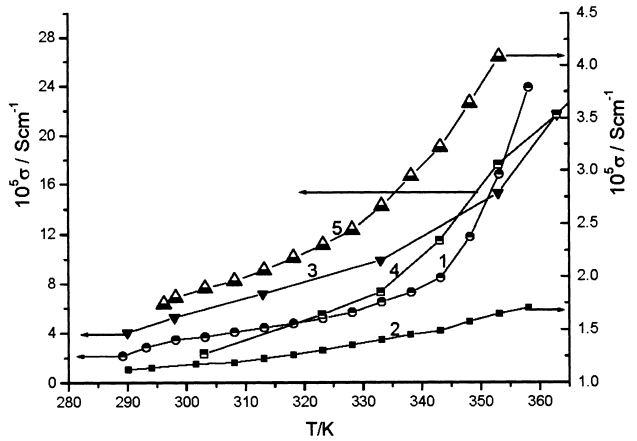

Fig. 7. Plot of temperature-dependent conductance of complexes **1**, **2**, **3**, **4** and **5**.

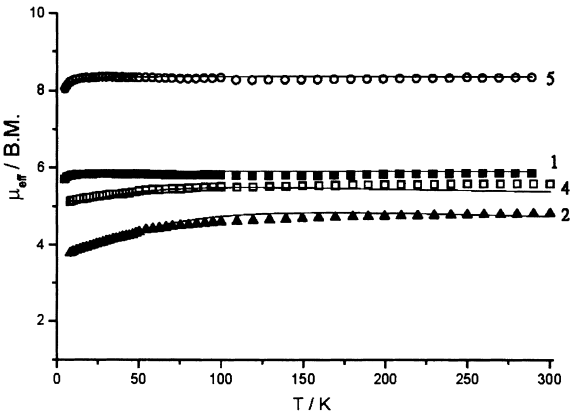

Fig. 8. Temperature dependence of the experimental effective magnetic moments (μ_{eff}) per MK_2 unit of complexes **1**, **2** and **4** and per Mn_2Na_2 unit of complex **5**. The solid lines represent the calculated values.

respectively, by analyzing the conductivity curves. The electrical conductivity of a complex as one piece of evidences has been provided to explain the weak interaction between the metal ions in extended solid structures.[20] It seems that the semi-conductivity of these complexes should be correlated to their common structural characteristic, such as alkali metal chains containing H_2O bridges in which the intermetallic separation is smaller than the sum of the van der Waals radii, showing the existence of a M_{alkali}–M_{alkali} weak interaction. A complex with a similar alkali metal chain, $[Na_2(\mu\text{-}OH)_2]_n$, has been reported to have a semiconductor feature.[21] Therefore, the alkali metal chains may provide a potential way to pass electricity. It is noted that complexes (**1**, **3**, **4**) containing K-chains have a higher conductivity than that of complex **5** containing Na-chains, which appear to be more disordered in the crystal structure when compared to the K-chains, and may decrease the ability to pass electricity. Some differences in the value of the electrical conducting properties between these complexes also imply that the transition-metal ions may also participate in the passage of electricity, and would concern its passage. Though it is difficult to explain why the Co/K complex (**2**) has the lowest conductivity, the adulteration of the Mn ion obviously increases the conductivity of complex **4**. Consequently, the influence of both the alkali and the transition metals on the electrical conductivity is indicated.

Magnetic Properties. Variable-temperature magnetic susceptibility measurements of **1**, **2**, **4**, and **5** were carried out in the range of 5–300 K. The temperature dependence of the experimental effective magnetic moments (μ_{eff}) for these complexes is shown in Fig. 8. The paramagnetic sites, Mn(II) and Co(II), in an octahedral environment are generally considered to be in a high spin state, $S = 5/2$ for Mn(II) and $S = 3/2$ for Co(II). Because of a too long separation of the M(II) centers (M = Mn, Co) to transfer magnetic interactions, the magnetic interactions between paramagnetic sites can be omitted. The magnetic behaviors of these complexes with the temperature variation should be attributed to a zero-field splitting of Mn(II) in the ground state ($^6A_{1g}$) for Mn complexes (**1**, **5**), or the actions of both the ligand field and the spin-orbit coupling for Co(II) complex **2**.

The following theoretical expression[22] for the zero-field splitting of $S = 5/2$ spin was used to fit the variable-temperature susceptibilities for **1** and **5**:

$$\chi_{Mn} = \frac{\chi_{II} + 2\chi_{\perp}}{3}, \quad (1)$$

$$\chi_{II} = \frac{Ng^2\beta^2}{4kT}\left[\frac{1 + 9\exp(-2D/kT) + 25\exp(-6D/kT)}{1 + \exp(-2D/kT) + \exp(-6D/kT)}\right],$$

$$\chi_{\perp} = \frac{Ng^2\beta^2}{4kT}\left[\frac{9 + 8/x - 11e^{-2x}/2x - 5e^{-6x}/2x}{1 + e^{-2x} + e^{-6x}}\right], \quad x = D/kT.$$

The actions of the ligand field and spin-orbit coupling for Co(II) can be expressed as follows, and was used for fitting the magnetic data of complex **2**.

$$\chi_{Co} = \frac{N\beta^2}{3kT}\left[\frac{A}{B}\right], \quad (2)$$

$$A = 3\left[\frac{7(3 - y)^2}{5} + \frac{12(2 + y)^2}{25yx} + \left\{\frac{2(11 - 2y)^2}{45} + \frac{176(y + 2)^2}{675yx}\right\} \times \exp\left(\frac{-5yx}{2}\right) + \left\{\frac{(y + 5)^2}{9} - \frac{20(y + 2)^2}{27yx}\right\} \times \exp(-4yx)\right]$$

$$B = 3 + 2\exp(-5yx/2) + \exp(-4yx),$$

$$x = \lambda/kT.$$

The following equation was used to fit the magnetic data of complex **4**:

$$\chi_M = \frac{\chi_{Mn} + \chi_{Co}}{2}, \quad (3)$$

where χ_{Mn} and χ_{Co} were calculated by Eq. 1 and Eq. 2, respectively.

A least-squares fitting of the experimental data for each complex led to $D = 2.1$ cm^{-1}, $g = 2.0$ and $R = 1.04 \times 10^{-4}$ for **1**, $D = 2.2$ cm^{-1}, $g = 2.0$ and $R = 8.7 \times 10^{-6}$ for **5** and $\lambda = -102.1$ cm^{-1}, $y = 1.15$, and $R = 1.23 \times 10^{-3}$ for **2**. Here, λ is the spin-orbit coupling parameter, y is a parameter representing the intensity of the ligand field, $1.0 < y < 1.5$ was considered to be reasonable[23] and R is the agreement factor, defined as $R = \Sigma[(\chi_M)_{obs} - (\chi_M)_{calcd}]^2/\Sigma[(\chi_M)_{obs}^2]$. According to the zero-field splitting of Mn(II) and the actions of both the ligand field and the spin-orbit coupling of Co(II), the fitting for complex **4** also gave a reasonable result: $D = 0.46$ cm^{-1}, $g =$

2, $\lambda = -65.3\ cm^{-1}$, $y = 1.31$, and $R = 1.25 \times 10^{-4}$.

Experimental

All manipulations were performed under aerobic conditions, and all commercially available reagents were used as received. IR spectra were recorded on a Magna-75-FT-IR spectrophotometer as KBr pellets (4000–400 cm^{-1}). The variable-temperature susceptibility was measured on a model CF-1 superconducting magnetometer with a crystalline sample kept in a capsule at 5–300 K. Diamagnetic corrections were made with Pascal's constants for all of the constituent atoms of the determined complexes. Elemental analyses were performed by a Germany Elemental Analyzer Vario EL Ⅲ.

$[MK_2(pdc)_2(H_2O)_7]_n$ (M = Mn(1), Co(2), Zn(3)): Dipicolinic acid (4 mmol) and KOH (8 mmol) were dissolved in 30 mL of a H_2O/CH_3OH solution (v/v, ca. 1:2). To the clear solution, $Mn(OAc)_2{\cdot}4H_2O$ (2 mmol) in 5 mL of H_2O was added dropwise with continuous stirring. The resulting yellow solution was allowed to stand for three weeks at 4 °C to give yellow prismatic crystals of **1** (yield, 91%). Anal. Calcd for $C_{14}H_{20}K_2MnN_2O_{15}$: C, 28.53; H, 3.42; N, 4.75; Mn, 9.32%; Found: C, 28.81; H, 3.24; N, 4.41; Mn, 9.25%. IR (KBr) 3454 (br s), 1628 (s), 1589 (s), 1379 (s), 1362 (s), 1277 (m), 1184 (m), 1078 (m), 1028 (m), 914 (m), 768 (s), 741 (s), 694 (m), 667 (s), 428 cm^{-1} (m). The preceding procedure was utilized to synthesize complexes **2**–**3** using the corresponding metal(Ⅱ) acetate instead. Similar IR data of complexes **2**–**3** to those of **1** were observed, and satisfactory elemental analyses were also obtained.

$[Mn_{0.5}Co_{0.5}K_2(pdc)_2(H_2O)_7]_n$ (4): The preceding procedure was utilized to synthesize complex **4** using $Mn(OAc)_2{\cdot}4H_2O$ (1 mmol) and $Co(OAc)_2{\cdot}4H_2O$ (1 mmol) as a transition-metal acetate. Green-blue block crystals of **4** were obtained (yield, 77%) after one week. Anal. Calcd for $C_{14}H_{20}Co_{0.5}K_2Mn_{0.5}N_2O_{15}$: C, 28.43; H, 3.41; N, 4.74; Mn, 4.64; Co, 4.98%; Found: C, 28.51; H, 3.35; N, 4.65; Mn, 4.78; Co, 5.07%. IR data of **4** were very close to those of **1**.

$\{[Na_2(H_2O)_8(CH_3OH)_{0.5}][Mn_2Na_2(C_7H_3NO_4)_4(H_2O)_8]\}_n$ (5): The replacement of KOH by NaOH in the procedure for preparation of **1** afforded a yellow powder, which was recrystallized from 20 mL of a H_2O/CH_3OH solution (v/v, ca 1:5) to give yellow prismatic crystals of **5** (yield, 64%) after two weeks. Anal. Calcd for $C_{28.5}H_{46}Mn_2N_4Na_4O_{32.5}$: C, 29.34; H, 3.97; N, 4.80; Na, 7.88; Mn, 9.42%; Found: C, 30.03; H, 3.01; N, 5.00; Na, 8.55; Mn, 9.98%. IR (KBr) 3539 (s), 3447 (s), 3232 (br s), 1639 (s), 1628 (s), 1610 (s), 1585 (s), 1429 (s), 1379 (s), 1277 (m), 1184 (m), 1076 (s), 1028 (m), 914 (m), 779 (s), 735 (m), 698 (m), 667 (m), 434 cm^{-1} (m). The crystals rapidly effloresce and may partly dehydrate when exposed to air, leading to an unsatisfactory elemental analysis result.

$[Ni(H_2O)_6][Ni_2K_2(pdc)_4(H_2pdc)_2(H_2O)_2]{\cdot}2H_2O$ (6): The reaction of H_2pdc (4 mmol) with KOH (8 mmol) and $NiSO_4{\cdot}4H_2O$ (2 mmol) in 20 mL of H_2O under stirring at room temperature for 1 h resulted in a blue solution. Slow diffusion of Et_2O vapor into the resulting solution produced blue-plate crystals of **6** (yield, 67%). Anal. Calcd for $C_{42}H_{42}K_2N_6Ni_3O_{34}$: C, 35.30; H, 2.96; N, 5.88; O, 38.06; K, 5.47; Ni, 12.32%; Found: C, 35.38; H, 2.89; N, 5.97; O, 38.30; K, 5.53; Ni, 12.18%. IR (KBr): 3521 (s), 3448 (br s), 3089 (s), 1714 (s), 1618 (s), 1591 (s), 1574 (s), 1443 (m), 1427 (s), 1398 (s), 1369 (m), 1356 (s), 1315 (s), 1281 (m), 1248 (s), 1186 (s), 1076 (s), 1038 (m), 1001 (m), 922 (m), 883 (m), 847 (m), 820 (s), 775 (s), 758 (m), 731 (s), 692 (s), 436 cm^{-1} (m).

Table 5. Crystallographic Data for Compounds **1**–**6**

Complex	**1**	**2**	**3**	**4**	**5**·0.25MeOH·2H_2O	**6**
Formula	$C_{14}H_{20}K_2MnN_2O_{15}$	$C_{14}H_{20}CoK_2N_2O_{15}$	$C_{14}H_{20}K_2N_2O_{15}Zn$	$C_{14}H_{20}Co_{0.5}K_2Mn_{0.5}N_2O_{15}$	$C_{28.75}H_{51}Mn_2N_4Na_4O_{34.75}$	$C_{42}H_{42}K_2N_6Ni_3O_{34}$
Fw	589.46	593.45	599.89	591.4525	1210.58	1429.15
Space group	*Pnna*	*Pnna*	*Pnna*	*Pnna*	*Pmc*2(1)	$P\bar{1}$
a/Å	20.653(1)	20.7074(4)	20.6905(9)	20.669(1)	43.7216(9)	10.8142(1)
b/Å	13.7610(2)	13.5235(3)	13.4868(3)	13.6306(3)	13.5320(1)	10.8956(1)
c/Å	8.1589(1)	8.2352(1)	8.1909(3)	8.1909(1)	8.5362(2)	12.4034(2)
α/deg	90	90	90	90	90	96.498(1)
β/deg	90	90	90	90	90	105.385(1)
γ/deg	90	90	90	90	90	104.128(1)
V/Å^3	2318.84(4)	2306.16(7)	2285.66(14)	2307.67(6)	5050.36(2)	1341.50(3)
Z	4	4	4	4	4	1
μ/mm^{-1}	1.004	1.181	1.516	1.180	0.639	1.308
D_{calcd}/g cm^{-3}	1.668	1.709	1.743	1.708	1.592	1.769
θ range/deg	1.97–25.02	1.97–24.99	1.97–25.06	1.97–25.02	0.93–25.13	1.73–25.03
Refls. [$I > 2\sigma(I)$]	1805	1733	1669	1705	4538	4044
R	0.0271	0.0336	0.0424	0.0363	0.0649	0.0525
R_w	0.0808	0.0965	0.1540	0.1048	0.1743	0.1394

X-ray Structure Determination. All of the crystals suitable for X-ray diffraction were selected from the reaction solutions for complexes **1**–**4** and **6**, while a single crystal of **5** was selected from liquid paraffin and sealed in a glass capillary to prevent decay. The diffraction data were collected on a Siemens SMART CCD diffractometer with graphite-monochromated Mo Kα radiation (λ = 0.71073 Å) using the ω-scan mode at 293 K. The intensity data were corrected for Lorentz-polarization factors, and an empirical absorption correction was applied. The structures were solved by direct methods and Fourier techniques for each compound and refined by a full-matrix least-squares calculation with SHELXL-97 program package[24] on a DELL computer. All the non-hydrogen atoms were refined anisotropically, except for those of the solvate methanol molecule in **5**, which were disordered in the lattice with an estimated occupancy of 0.25. The alkali metal atoms Na3, Na4, Na5 and Na6 locate at the respective position with the crystallographically defined occupancy of 0.5 for each. Hydrogen atoms were introduced geometrically, except for those of water molecules in **1**, **2** and **6**, which were located from the difference Fourier syntheses. No attempt was made to add hydrogen atoms to water and methanol molecules in **3**–**5**. A summary of the crystallographic data is compiled in Table 5.

This work was supported by State Key Basic Research and Development Plan of China (G1998010100), the NNSFC (29973047, 30170229 and 39970177) and Expert Project of Key Basic Research from Ministry of Sci. & Tech.

References

1 a) G. Chessa, G. Marangoni, B. Pitteri, V. Bertoasi, G. Gilli, and V. Ferreti, *Inorg. Chem. Acta*, **185**, 201 (1991). b) A. M. Herring, L. Henling, J. A. Labinger, and J. E. Bercaw, *Inorg. Chem.*, **30**, 851 (1991).

2 a) M. G. B. Drew, G. W. A. Fowles, R. W. Matthews, and R. A. Walton, *J. Am. Chem. Soc.*, **91**, 7769 (1969). b) P. P. Quaglieri, H. Loiseleur, and G. Thomas, *Acta Crystallogr., Sect. B*, **28**, 2583 (1972). c) P. Lainé, A. Gourdon, and J.-P. Launay, *Inorg. Chem.*, **34**, 5156 (1995).

3 a) K. J. Palmer, R.-Y. Wong, J. C. Lewis, *Acta Crystallogr., Sect. B*, **28**, 223 (1972). b) G. Nardin, L. Randaccio, R. P. Bonomo, and E. Rizzarelli, *J. Chem. Soc., Dalton Trans.*, **1980**, 369. c) P. Starynowicz, *Acta Crystallogr., Sect. C*, **48**, 1428 (1992). d) S. K. Sengupta, S. K. Shani, and R. N. Kapoor, *Polyhedron*, **2**, 317 (1983). e) A. Yu. Lenotiev, M. D. Arion, I. M. Razdobreev, G. A. Kiosse, Yu. V. Yablokov, T. I. Malinovskii, and G. A. Popovich, *Dokl. Akad. Nauk SSSR*, **300**, 1129 (1988).

4 a) B. S. Church and H. Halvorson, *Nature*, **183**, 124 (1959). b) G. F. Bailey, S. Karp, and T. E. Sacks, *J. Bacteriol.*, **89**, 984 (1965). c) L. Chung, K. S. Rajan, E. Merdinger, and N. Greez, *Biophys. J.*, **11**, 469 (1971). d) G. Scapin, S. G. Reddy, R. Zheng, and J. S. Blanchard, *Biochemistry*, **36**, 15081 (1997).

5 a) D. L. Hoof, D. G. Tisley, and R. A. Walton, *J. Chem. Soc., Dalton Trans.*, **1973**, 200, and references therein. b) M. Chatterjee, M. Maji, S. Ghosh, and T. C. W. Mak, *J. Chem, Soc., Dalton Trans.*, **1998**, 3641.

6 a) C. Sheu and D. T. Sawyer, *J. Am. Chem. Soc.*, **112**, 8212 (1990). b) L. Morimoto and S. Tanaka, *Anal. Chem.*, **35**, 1234 (1963). c) C. G. Pope, E. Matijevic, and R. C. Patel, *J. Colloid Interface Sci.*, **80**, 874 (1981). d) Y. Pocker and C. T. O. Fong, *Biochemistry*, **19**, 2045 (1980).

7 a) M. Ohba and H. Okawa, *Coord. Chem. Rev.*, **198**, 313 (2000). b) J. Lisowski and P. Starynowicz, *Inorg. Chem.*, **38**, 1351 (1999). c) M. Andruh, I. Ramade, E. Codjovi, O. Guillou, O. Kahn, and J.-C. Trombe, *J. Am. Chem. Soc.*, **115**, 1822 (1993). d) C. Mathonière, C. J. Nuttall, S. G. Carling, and P. Day, *Inorg. Chem.*, **35**, 1201 (1996).

8 a) R. H. Holm, P. Kennepohl, and E. I. Solomon, *Chem. Rev.*, **96**, 2239 (1996). b) A. Zouni, H.-T. Witt, J. Kern, P. Fromme, N. Krauß, W. Saenger, and P. Orth, *Nature*, **409**, 739 (2001).

9 a) W. E. Rhine, R. B. Hailock, W. M. Davis, and W. Wong-Ng, *Chem. Mater.*, **4**, 1208 (1992). b) S. Decurtins, H. W. Schmalle, R. Pellaux, P. Schneuwly, and A. Hauser, *Inorg. Chem.*, **35**, 1451 (1996). c) S. Decurtins, H. W. Schmalle, P. Schneuwly, J. Ensing, and P. Gütlich, *J. Am. Chem. Soc.*, **116**, 9521(1994). d) R. Pellaux, H. W. Schmalle, R. Huber, P. Fischer, T. Hauss, B. Ouladdiaf, and S. Decurtins, *Inorg. Chem.*, **36**, 2301 (1997). e) M. McComack, S. Jin, T. H. Tiefel, R. M. Fleming, and J. M. Phillips, *Appl. Phys. Lett.*, **64**, 3045 (1994).

10 A. S. Johnson, P. J. Olliver, and T. E. Mallouk, *Science*, **283**, 963 (1999).

11 a) M. A. Withersby, A. J. Blake, N. R. Champness, P. Hubbersty, W.-S. Li, and M. Schröder, *Angew. Chem., Int. Ed. Engl.*, **36**, 2327 (1997). b) L. Carlucci, G. Ciani, D. M. Proserpio, and A. Sironi, *Angew. Chem., Int. Ed. Engl.*, **34**, 1895 (1995). c) R. Vilar, D. M. P. Mingos, A. J. P. White, and D. J. Williams, *Angew. Chem., Int. Ed.*, **37**, 1258 (1998). d) M.-L. Tong, B.-H. Ye, J.-W. Cai, X.-M. Chen, S. and W. Ng, *Inorg. Chem.*, **37**, 2645 (1998).

12 D. M. J. Doble, C. H. Benison, A. J. Blake, D. Fenske, M. S. Jackson, R. D. Kay, W.-S. Li, and M. Schröder, *Angew. Chem., Int. Ed.*, **38**, 1915 (1999).

13 A. J. Bondi, *Phys. Chem.*, **68**, 441 (1964).

14 B. R. McGarvey, "ESR of Transition Metal Complexes," in "Transition Metal Chemistry, Vol. 3," New York (1967).

15 C. Ma, W. Wang, H. Zhu, C. Chen, and Q. Liu, *Inorg. Chem. Commoun.*, **4**, 730 (2001).

16 N. Okabe and N. Oya, *Acta Crystallogr., Sect. C*, **56**, 305 (2000).

17 a) P. Laine, A. Gourdon, and J.-P. Launay, *Inorg. Chem.*, **34**, 5129 (1995), and references therein. b) A. G. Mauk, E. Bordignon, and H. B. Gray, *J. Am. Chem. Soc.*, **104**, 7654 (1982). c) G. Balavoine, D. H. R. Barton, A. Gref, and L. Lellouche, *Tetrhedron*, **48**, 1883 (1992). d) J. T. Groves and I. O. Kady, *Inorg. Chem.*, **32**, 3868 (1993).

18 G. B. Deacon and R. J. Philips, *Coord. Chem. Rev.*, **33**, 227 (1980).

19 C. Kettel, "Solid State Physics," 5th ed, John Wiley & Sons Inc., New York (1976).

20 M. Jansen, *Angew. Chem. Int. Ed. Engl.*, **26**, 1098 (1987).

21 Y. Chen, Q. Liu, Y. Deng, H. Zhu, C. Chen, H. Fan, D. Liao, and E. Gao, *Inorg. Chem.*, **40**, 3725 (2001).

22 O. Kahn, "Molecular Magnetism," VIH, New York (1993).

23 E. A. Boudreaux and L. N. Mulay, "Theory and Applications of Molecular Paramagnetism," John Wiley & Sons, New York (1976).

24 G. M. Sheldrick, "SHELXL-97," Universität Göttingen (1997).